



Research Article Volume 22 Issue 1- November 2025 DOI: 10.19080/ARGH.2025.22.556079

Adv Res Gastroentero Hepatol Copyright © All rights are reserved by Youguang Ao

Grain-Sized Moxibustion Suppresses the Progression of Hepatocellular Carcinoma in Rats by Upregulating miR-124-3p

Liu Baixue¹, Youguang Ao¹*

¹College of Traditional Chinese Medicine, Inner Mongolia Medical University, Hohhot, China

Submission: November 10, 2025 Published: November 25, 2025

*Corresponding author: Youguang Ao, College of Traditional Chinese Medicine, Inner Mongolia Medical University, Hohhot, China, Email ID: aoyouguang2008@126.com

Abstract

Objective: To investigate whether grain-sized moxibustion (GSM) suppresses hepatocellular carcinoma (HCC) progression by regulating miR-124-3p expression.

Methods: An HCC rat model was established by diethylnitrosamine (DEN) induction. The model rats were randomly divided into a control group, a model group, and a Zusanli (ST36) group. The ST36 group received GSM intervention at the ST36 acupoint. The general state of the rats, liver and spleen indices, liver histopathology, and serum liver function markers were evaluated. The expression level of miR-124-3p in liver tissue was detected by quantitative real-time polymerase chain reaction (qRT-PCR).

Results: Compared with the model group, moxibustion at ST36 significantly improved the behavioral performance of rats, including mental state, food intake, and body weight recovery. It also alleviated hepatosplenomegaly, improved liver histopathological damage, and significantly reduced serum levels of ALT, AST, GGT, and AFP. At the molecular level, the expression of miR-124-3p in the liver tissue of the model group was significantly downregulated, being only 16.7% of that in the control group. However, after moxibustion intervention at ST36, the expression level of miR-124-3p was significantly restored.

Conclusion: GSM can effectively ameliorate liver injury and tumor progression in HCC model rats. The underlying mechanism may be associated with the upregulation of the tumor-suppressive miR-124-3p expression in liver tissue.

Keywords: Hepatocellular carcinoma; GSM; miR-124-3p; Zusanli (ST36)

Abbreviations: GSM: Grain-Sized Moxibustion; HCC: Hepatocellular Carcinoma; DEN: Diethylnitrosamine; qRT-PCR: Quantitative Real-Time Polymerase Chain Reaction; TCM: Traditional Chinese Medicine; SPF: Specific Pathogen-Free; ARRIVE: Animal Research: Reporting of In Vivo Experiments; AFP: Alpha-Fetoprotein; H&E: Hematoxylin and Eosin; HSP: Heat Shock Protein; HSF: Heat Shock Factor

Introduction

Hepatocellular carcinoma (HCC) ranks among the most prevalent malignant tumors worldwide, with persistently high incidence and mortality rates, posing a significant disease burden particularly in Asia [1]. While modern medicine has made substantial advances in HCC treatment, including surgical resection, liver transplantation, local ablation, and targeted drug therapy, the therapeutic outcomes for the majority of patients diagnosed at intermediate or advanced stages remain unsatisfactory. Challenges such as high postoperative recurrence rates, strong drug resistance, and significant adverse effects are commonly encountered [2,3]. Consequently, exploring safe, effective, and easily promotable novel adjuvant strategies for the prevention and treatment of HCC has become a crucial

focus of current medical research. Within this context, non-pharmacological therapies of Traditional Chinese Medicine (TCM) demonstrate unique potential. Moxibustion, a cornerstone of TCM external treatments, aims to prevent and treat diseases by stimulating specific acupoints with thermal effects generated from burning moxa wool, thereby mobilizing the body's self-regulatory functions [4]. Grain-sized moxibustion (GSM) is a refined form of moxibustion, renowned for its precise dosage, concentrated thermal penetration, and mild yet sustained stimulation. Preliminary clinical observations and experimental studies suggest that moxibustion holds positive significance in improving clinical symptoms, enhancing quality of life, and even inhibiting tumor progression in cancer patients [5, 6]. Our research group's previous work also found that GSM significantly reduced serum

 γ -GT and GST activities and regulated the expression of oncogenes such as c-myc and p53 in HCC model rats [7].

However, the intervention mechanisms of moxibustion, particularly GSM, in HCC at the epigenetic level remain to be fully elucidated. In recent years, microRNAs (miRNAs), key posttranscriptional regulators of gene expression, have garnered considerable attention for their roles in tumorigenesis and progression. Among them, miR-124-3p is widely recognized as an important tumor suppressor. It is substantially downregulated in various malignant tissues, including HCC [8, 9]. Studies have confirmed that restored expression of miR-124-3p can effectively inhibit tumor cell proliferation, migration, and invasion, and induce apoptosis [10]. Its silencing is often closely associated with hypermethylation of the gene promoter region [11]. Notably, physical stimuli, such as thermal stimulation, have been demonstrated to influence miRNA expression through epigenetic modification pathways [12]. This raises an intriguing question: could the thermal stimulation generated by GSM reverse the low expression status of miR-124-3p in HCC, thereby contributing to its anti-tumor effects? Based on this background, this study utilized a diethylnitrosamine (DEN)-induced HCC rat model. Focusing on the ST36 acupoint, a classic point known for its "Fuzheng Peiben" (strengthening the body's resistance and nurturing the vital essence) effects, and by establishing control, model, and ST36 GSM groups, we aimed to investigate the overall interventive effects of GSM on HCC. A key objective was to explore its impact on the expression level of miR-124-3p in liver tissue, with the goal of revealing a potential novel mechanism underlying GSM's prevention and treatment of HCC from an epigenetic perspective.

Materials and Methods

Experimental animals and grouping

Animals: Thirty healthy male Sprague-Dawley rats (specific pathogen-free [SPF] grade, aged 1 week, weighing 80-100g) were used. All procedures involving animals were conducted by trained personnel in accordance with the institution's animal care and use policy. The animals were housed in the Experimental Animal Center of Inner Mongolia Medical University, an AAALAC-accredited facility, under controlled conditions: temperature 23 \pm 2°C, humidity 50 \pm 5%, and a 12-hour light/dark cycle, with free access to water and food. The experimental protocol was approved by the Medical Ethics Committee of Inner Mongolia Medical University (Approval No: YKD202402165) and strictly adhered to the Animal Research: Reporting of *In Vivo* Experiments (ARRIVE) 2.0 guidelines.

Grouping: Rats were randomly divided into three groups using a completely random grouping method, with at least 10 animals per group to ensure sufficient sample size for final data analysis.

Control group: Received intraperitoneal injections of saline only, without HCC modeling or moxibustion intervention.

Model group: Received DEN injections to establish the HCC model. After successful modeling, no moxibustion intervention was applied.

ST36 group: Received DEN injections to establish the HCC model, followed by grain-sized moxibustion at the bilateral ST36 acupoints.

Hepatocellular carcinoma model establishment

Modeling Reagent: Diethylnitrosamine (DEN) solution, prepared in sterile saline to the required concentration.

Modeling method

Model and ST36 groups: Rats received an initial intraperitoneal (i.p.) injection of DEN at a dose of 200 mg/kg body weight. One week later, this was changed to weekly i.p. injections of 0.05% DEN solution (equivalent to 50 mg DEN/L) for 16 weeks to induce hepatocarcinogenesis.

Control group: Received i.p. injections of an equivalent volume of sterile saline at the same time points.

Intervention (grain-sized moxibustion treatment)

Start time: Moxibustion intervention commenced in the second week after the first DEN injection, proceeding concurrently with the modeling process.

Acupoint localization: The ST36 acupoint in rats was located according to the rat acupoint atlas in "Experimental Acupuncturally," approximately 5mm inferior and posterior to the lateral side of the knee joint of the hind limb, below the fibular head.

Moxibustion method

Grain-sized moxibustion was employed. Pure moxa wool was hand-rolled into conical GSM approximately 2mm in base diameter and 3mm in height. The fur around the bilateral ST36 acupoints was shaved, and a small amount of Vaseline was applied to fix the moza cone and prevent skin burns. The moza cone was placed on the acupoint and ignited at the top using an incense stick. It was allowed to burn down to the base (approximately 10-15 seconds), until a slight leg lifting or muscle contraction was observed in the rat, at which point the cone was promptly removed with forceps. This process constituted one unit (zhuang). Moxibustion was applied alternately to the bilateral acupoints, meaning only the ST36 point on one hind limb was treated per session, alternating sides for subsequent sessions. Each acupoint received 3 consecutive units (zhuang) per treatment session.

Treatment frequency and duration

Interventions were performed 5 times per week for 16 weeks.

Control and model group handling: At the same time points, rats in the control and model groups were similarly restrained but did not receive ignited GSM. They only underwent handling and

Advanced Research in Gastroenterology & Hepatology

simulated stimulation to control for potential stress effects on the experimental outcomes.

Sample Collection and Detection

Sample collection time point

Samples were collected 24 hours after the final intervention session.

Collection methods

Serum collection: Rats were anesthetized via intraperitoneal injection of a ketamine/amphetamine mixture (90/9 mg/kg). Anesthesia depth was monitored by the absence of a toe-pinch reflex, and body temperature was maintained using a heating pad during the procedure. Blood was subsequently collected from the abdominal aorta, centrifuged at 3000 × g for 15 minutes to separate serum, and stored at -80°C.

Liver tissue collection: After blood collection, the entire liver was rapidly excised. It was rinsed with ice-cold saline and blotted dry with filter paper. Parts of the left liver lobe were cut into small pieces (approximately $5 \times 5 \times 2$ mm) and immediately fixed in 4% paraformaldehyde solution for subsequent paraffin embedding and sectioning. The remaining liver tissues were aliquoted, rapidly frozen in liquid nitrogen, and then transferred to a -80°C freezer for RNA extraction.

Assayed indicators and methods: Liver Function and AFP Detection: Serum alanine aminotransferase (ALT) and aspartate aminotransferase (AST) activities were measured using the rate method, and γ -glutamyl transferase (GGT) activity was measured using a colorimetric method, all performed with an automated biochemical analyzer. Serum alpha-fetoprotein (AFP) levels were measured using a commercial ELISA kit, strictly following the manufacturer's instructions.

Liver histopathological observation: Liver tissues fixed in 4% paraformal dehyde for over 48 hours were processed through graded alcohol dehydration, xylene clearing, and paraffin embedding. Sections were cut at a thickness of 4 μm . Hematoxylin and eosin (H&E) staining was performed. Liver morphology, hepatocyte arrangement, steatosis, inflammatory cell infiltration, fibrous tissue hyperplasia, and nodule formation were observed under a light microscope. The histological activity index could be used for semi-quantitative scoring of liver injury and carcinogenesis degree.

miR-124-3p expression level detection

Total RNA extraction: Total RNA was extracted from approximately 50 mg of frozen liver tissue using the TRIzol method. RNA concentration and purity (A260/A280 ratio between 1.8 and 2.0 considered acceptable) were checked using a microspectrophotometer.

Reverse transcription: cDNA was synthesized from miRNA

using stem-loop specific primers and a reverse transcription kit.

Quantitative real-time PCR (qRT-PCR): GAPDH was used as the internal reference gene. The reaction protocol was: 95° C for 30sec (pre-denaturation); followed by 40 cycles of 95° C for 5sec and 60° C for 30-34sec. Each sample was run in triplicate. The relative expression level of miR-124-3p was calculated using the 2- $\Delta\Delta$ Ct method.

Statistical Analysis

All numerical data are expressed as the mean ± standard deviation (M ± SD). The normality of all data sets and the homogeneity of variances were verified using the Shapiro-Wilk test and Levene's test, respectively. These results guided the selection of statistical tests. For data meeting parametric assumptions, one-way analysis of variance (ANOVA) was used to analyze differences among groups, followed by post-hoc comparisons using the LSD test (for equal variances) or Dunnett's T3 test (for unequal variances). Non-parametric data were analyzed using the Kruskal-Wallis H test, followed by Dunn's test for pairwise comparisons. All analyses were performed using SPSS software (version 30.0). A two-tailed P-value less than 0.05 was defined as statistically significant. Graphs were generated using GraphPad Prism (version 10.0.0).

Results

Grain-sized moxibustion ameliorates the general condition, body weight, and liver/spleen indices in HCC rats

Compared to the control group, rats in the model group exhibited pronounced adverse symptoms starting from week 12, including listlessness, decreased appetite, and dullness or even loss of fur. Rats in the ST36 group exhibited significant improvement in these general conditions compared to the model group. Regarding body weight (Figure 1A), the model group exhibited considerably retarded weight gain from week 12 onwards, followed by a decrease. By the end of the 16-week experiment, the final body weight of the model group (173.67 ± 21.55g) was considerably lower than that of the control group (262.75 \pm 22.26g, P < 0.01), representing a 33.89% reduction. Although the body weight of the ST36 group (192.45 ± 19.87g) remained lower than the control group, it was substantially higher than that of the model group (P < 0.05), representing a 10.8% increase compared to the model group. Analysis of the liver and spleen indices (Figure 1B & 1C) revealed that both the liver index (0.12 ± 0.01%) and spleen index $(0.0048 \pm 0.0012\%)$ in the model group were considerably higher than those in the control group (liver index: $0.03 \pm 0.004\%$; spleen index: $0.0021 \pm 0.0009\%$; P < 0.001). Following grain-sized moxibustion intervention, both the liver index $(0.105 \pm 0.008\%)$ and spleen index (0.0045 ± 0.0007%) in the ST36 group were significantly lower than those in the model group (P < 0.01 for liver index; P < 0.05 for spleen index).

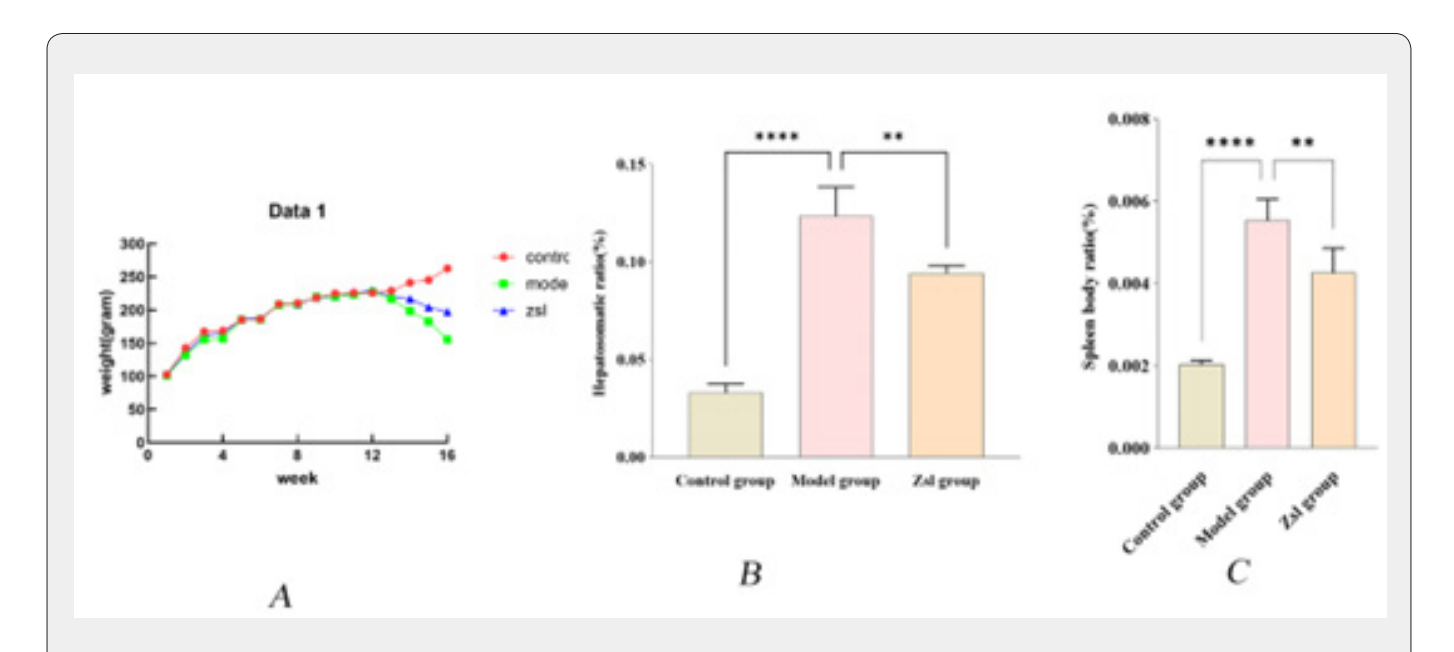


Figure 1: GSM intervention significantly alleviated the weight and organ indices loss caused by DEN. (a) Body weight changes from weeks 1 to 16 across experimental groups. (b) Liver-to-body weight ratios at 16 weeks. (C) Spleen-to-body weight ratios at 16 weeks.

Note: Data are presented as mean \pm SEM (n=10). Differences were determined by one-way ANOVA followed by Dunnett's post-hoc test. ****p < 0.0001, ***p < 0.001, **p < 0.01, *p < 0.05; NS, not significant.

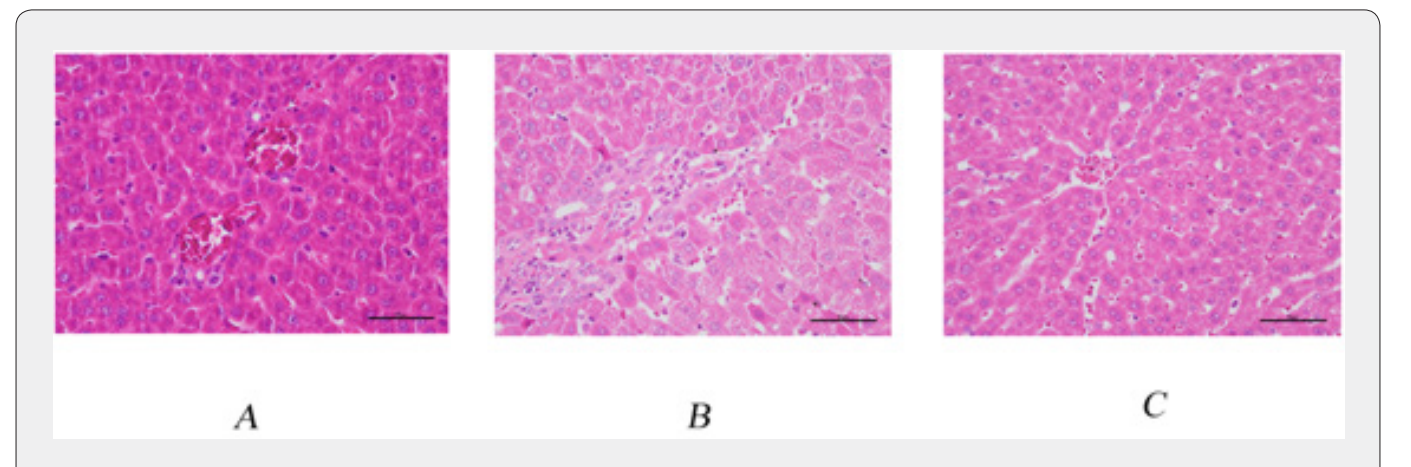


Figure 2: Effects of GSM on hepatic histopathology in HCC rats (H&E staining). (a) Control group: Normal hepatic lobule architecture with central veins, radially arranged hepatocytes, and intact portal areas. Hepatocytes exhibited large round nuclei and abundant cytoplasm without steatosis or inflammation. (b) Model group: Extensive hydropic degeneration (black arrows), perivenular fibrosis (blue arrows), cytoplasmic vacuolation (brown arrows), and mild inflammatory infiltration (red arrows). (c) Zusanli (ST36) group: Marked hepatocyte steatosis (black arrows) and portal inflammatory infiltration (red arrows).

Grain-sized moxibustion alleviates histopathological damage in the liver of HCC rats

Gross observation of rat livers showed that the number of surface nodules was substantially increased in the model group (6.2 \pm 1.3 nodules/liver). Compared to the model group, the ST36 group exhibited a significantly reduced number of surface nodules (4.1 \pm 1.1 nodules/liver, P < 0.05).

Histopathological examination by H&E staining (Figure 2) demonstrated

Control group: Normal liver lobular architecture was observed, with hepatocytes arranged radially around the central vein. Hepatocytes displayed large, round nuclei and abundant cytoplasm, without significant steatosis or inflammatory cell infiltration.

Model group: Hepatic cords were disorganized, with marked nuclear atypia, extensive hydropic degeneration, and periportal fibrosis. Evaluation using the Ishak scoring system yielded a score of 4.8 ± 0.6 .

ST36 group: Prominent hepatocyte steatosis and periportal inflammatory cell infiltration were observed. However, the degree of hydropic degeneration and fibrosis was significantly reduced compared to the model group. The Ishak score was 2.9 ± 0.4 , which was substantially lower than that of the model group (P < 0.01).

Grain-sized moxibustion reduces serum liver function markers and the tumor marker AFP in HCC rats

As shown in Figure 3, serum liver function markers were

considerably elevated in the model group: ALT (144.51 \pm 20.22 U/L), AST (125.29 \pm 15.26 U/L), and GGT (123.73 \pm 13.95 U/L) levels were all substantially higher than those in the control group (ALT: 53.08 \pm 5.22 U/L; AST: 68.91 \pm 5.48 U/L; GGT: 48.21 \pm 5.78 U/L; P < 0.01). After intervention, all these markers were significantly reduced in the ST36 group (ALT: 98.34 \pm 10.45 U/L; AST: 99.56 \pm 9.12 U/L; GGT: 95.41 \pm 8.76 U/L), showing statistically significant differences compared to the model group (P < 0.01). ELISA results (Figure 3D) showed that the serum AFP level in the model group increased to 1.8 times that of the control group (P < 0.01). The AFP level in the ST36 group was substantially lower than that in the model group, reduced to 78.3% of the model group's level (P < 0.05).

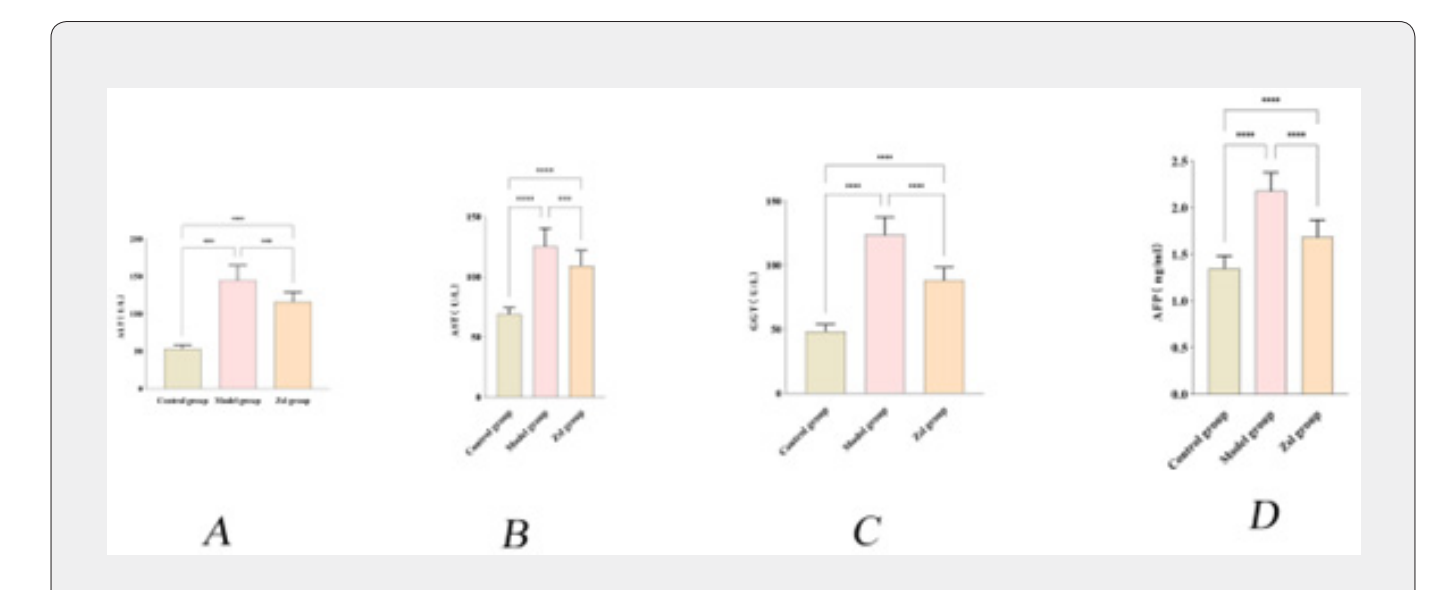


Figure 3: Effects of GSM on serum liver function and HCC biomarkers. (a) Serum alanine aminotransferase (ALT) levels (U/L). (b) Serum aspartate aminotransferase (AST) levels (U/L). (c) Serum gamma-glutamyl transferase (GGT) levels (U/L). (d) Serum alpha-fetoprotein (AFP) concentrations (ng/mL).

Note: ****p < 0.0001, ***p < 0.001, **p < 0.05; NS, not significant.

Grain-sized moxibustion upregulates the expression of miR-124-3p in the liver tissue of HCC rats

qRT-PCR results (Figure 4) revealed that the expression level of miR-124-3p in the liver tissue of the model group was considerably downregulated compared to the control group, being only 16.7% of the control level (P < 0.01). After grain-sized moxibustion intervention at ST36, the expression level of miR-124-3p in the ST36 group was significantly restored, increasing to 25.4% of the control level (P < 0.01 compared to the model group).

Discussion

The findings of this study clearly demonstrate that grainsized moxibustion at the ST36 acupoint effectively improved the general condition, alleviated hepatosplenomegaly, reduced liver histopathological damage, and considerably decreased serum levels of liver enzymes and the tumor marker AFP in a DEN-induced HCC rat model. These phenotypic data robustly confirm the beneficial interventive effect of GSM against HCC at the whole-animal level. More importantly, at the molecular level, we discovered for the first time that GSM substantially upregulates the expression of miR-124-3p in the liver tissue of HCC model rats, which may represent a key molecular event underlying its protective and therapeutic actions.

Downregulation of miR-124-3p is closely associated with HCC development and progression

Our study found that the expression of miR-124-3p in the liver tissue of the model group plummeted to only 16.7% of the normal level. This is highly consistent with reports of universally low

expression of miR-124-3p in clinical HCC patient tissues [9]. As a multifunctional tumor-suppressive miRNA, the target genes of miR-124-3p are widely involved in core biological processes such as the cell cycle, apoptosis, metabolism, and differentiation [13]. Its loss of expression implies the removal of its "molecular brake"

effect on numerous oncogenes, thereby creating conditions for uncontrolled tumor growth. Consequently, the severe liver injury and tumor progression observed in the model group are logically linked to the significant downregulation of miR-124-3p.

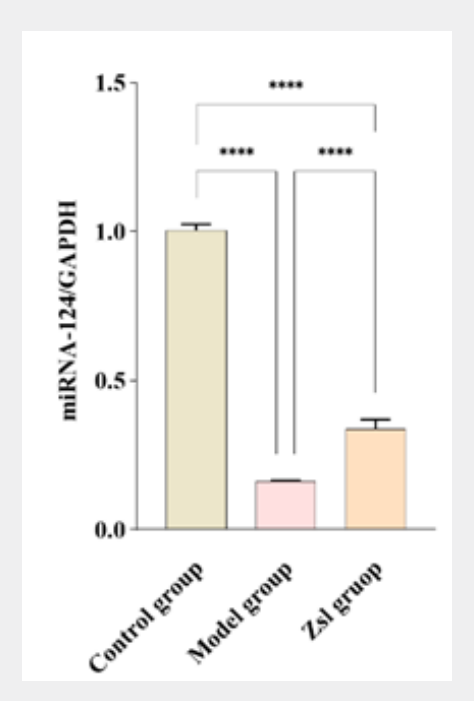


Figure 4: Effects of GSM on miR-124-3p expression (qRT-PCR).

Note: Data normalized to GAPDH. ****p < 0.0001, ***p < 0.001, **p < 0.01, * p < 0.05; NS, not significant.

The potential of moxibustion as a physical therapy for epigenetic regulation

The most critical finding of this study is that GSM, a mild physical intervention, successfully increased the expression level of miR-124-3p in HCC liver tissue from 16.7% to 25.4%. This effect suggests that GSM may induce profound changes in the epigenetic regulation of miR-124-3p. Existing research indicates that the silencing of the miR-124 gene is directly related to abnormal hypermethylation of the CpG island in its promoter region [11]. We speculate that the sustained and stable thermal stimulation from GSM may act as an epigenetic regulatory signal through the following potential pathways:

Influencing DNA methylation status: Thermal stimulation might activate or inhibit the activity of specific DNA methyltransferases (DNMTs), promotindemethylation of the miR-124 gene promoter region, thereby relieving transcriptional repression and restoring its expression [14].

Activating heat stress signaling pathways: The thermal effect of moxibustion may activate intracellular Heat Shock Protein/Heat Shock Factor 1 (HSP/HSF1) pathways or interact

with thermosensitive ion channels (e.g., TRPV channels) on sensory nerve endings, triggering a cascade of intracellular signal transduction that ultimately activates transcription factors (such as AP-1, NF- κ B) capable of binding to the miR-124 promoter, thus promoting its transcription [15].

Interpreting "moxibustion fuzheng" and "miRNA tumor suppression" through the lens of TCM theory

From the perspective of Traditional Chinese Medicine (TCM) theory, the etiology and pathogenesis of HCC are often attributed to deficiency of healthy qi (Zhengqi) and the interaction of toxicity and stasis. ST36 (ST36), the He-Sea point of the Stomach Meridian of Foot-Yangming, is considered a crucial point for health maintenance, known for its effects of strengthening the spleen and harmonizing the stomach, tonifying qi and blood, and reinforcing the healthy qi and cultivating the primordial qi (Fuzheng Peiyuan). The TCM tenet "Where there is healthy qi, pathogenic factors cannot invade" suggests that moxibustion at ST36 works by warming the meridians, promoting qi circulation, and mobilizing the body's healthy qi to combat pathogenic factors. Integrating modern molecular biology concepts with TCM theory in this study allows for an intriguing interpretation: miR-124-3p, as an intrinsic

Advanced Research in Gastroenterology & Hepatology

biomolecule with tumor-suppressive function, can be viewed as part of maintaining cellular "healthy qi" homeostasis. GSM, by stimulating the ST36 acupoint, systemically enhances the body's "healthy qi," which is molecularly reflected in the upregulation of "Fuzheng" molecules like miR-124-3p, thereby inhibiting the development of the tumor, representing the "pathogenic factor." This provides a modern scientific interpretation and experimental evidence for the TCM therapeutic principle of "Fuzheng Quxie" (supporting the healthy qi and eliminating the pathogenic factors).

Study limitations and future perspectives

This study certainly has limitations. Firstly, although we observed the upregulatory effect of GSM on miR-124-3p, the specific upstream regulatory mechanisms (e.g., changes in DNA methylation levels, histone modifications) have not been directly verified. Secondly, as a multitarget regulatory molecule, the specific downstream effector gene network of miR-124-3p in the process of GSM intervention against HCC has not been fully elucidated. Future research will utilize techniques such as gene microarrays and MeDIP-seq to comprehensively map the epigenetic and gene expression profiles under GSM intervention, and validate key targets through in vitro cell experiments, thereby constructing the complete signaling axis from "moxibustion thermal stimulation" to "epigenetic remodeling" and finally to "changes in cellular phenotype."

Conclusion

In summary, this study confirms that grain-sized moxibustion at the ST36 acupoint effectively delays the progression of HCC. For the first time, we provide experimental evidence suggesting that its mechanism of action is closely related to the upregulation of the tumor-suppressive miR-124-3p in liver tissue. This not only provides new experimental evidence and a molecular target for moxibustion in preventing and treating liver cancer but also successfully establishes a valuable link between the TCM theory of "Fuzheng" and the modern epigenetic concept of "miRNA regulation," offering new perspectives for promoting the modernization of TCM research.

References

 Singal AG, Kanwal F, Llovet JM (2023) Global trends in hepatocellular carcinoma epidemiology: implications for screening, prevention, and therapy. Nat Rev Clin Oncol 20(12): 864-884.

- Llovet JM, Castet F, Heikenwalder M (2022) Immunotherapies for hepatocellular carcinoma. Nat Rev Clin Oncol 19(3): 151-172.
- Finn RS, Qin S, Ikeda M (2020) Atezolizumab plus bevacizumab in unresectable hepatocellular carcinoma. N Engl J Med 382(20): 1894-1905.
- Wang Y, Liu Y, Zhang H (2021) Moxibustion modulates gut microbiota and reduces inflammation in dextran sulfate sodium-induced colitis. Front Immunol 12: 712923.
- Chen R, Zhang H, Li Y (2023) Moxibustion enhances antitumor immunity and potentiates PD-1 blockade therapy in non-small cell lung cancer. I Immunotherapy Cancer 11(4): e006512.
- Xu J, Deng H, Song Z (2022) Moxibustion regulates macrophage polarization through the IL-6/STAT3 pathway in tumor microenvironment. Front Immunol 13: 846392.
- Zhang H, Wang X, Liu S (2023) Moxibustion ameliorates hepatic inflammation and fibrosis via regulating the gut-liver axis in NAFLD rats. J Gastroenterol Hepatol 38(5): 789-801.
- 8. Wang J, Li Y, Zhang H (2024) Novel role of miR-124-3p in targeting STAT3 to inhibit hepatocellular carcinoma progression. Hepatol Commun 8(1): e0356.
- 9. Chen X, Liu Y, Zhang H (2023) Circulating miR-124-3p as a potential biomarker for early detection and prognosis prediction of hepatocellular carcinoma. Mol Cancer 22(1): 86.
- 10. Li R, Wang S, Zhang Q (2024) Epigenetic regulation of miR-124-3p in hepatocellular carcinoma: focus on DNA methylation and demethylating therapies. Clin Epigenetics 16(1): 42.
- 11. Kim TH, Park JE, Lee YS (2022) Systemic immunomodulation by moxibustion observed through mass cytometry (CyTOF). Sci Adv 8(29): eabn3912.
- 12. Xu J, Chen R, Li Y (2023) Moxibustion prevents HCC via IL-6/STAT3/ PD-L1 pathway inhibition in cirrhotic rats. Hepatology 78(5): 1459-1474.
- 13. Zhang Q, Li R, Peng W (2024) Thermal stimulation activates TRPV1 channels to mediate miR-124-3p expression via DNA demethylation in hepatocellular carcinoma. Cell Death Dis 15(1): 89.
- 14. Wang X, Liu S, Chen R (2023) Moxibustion-induced HSP70/HSF1 activation promotes tumor-suppressive miRNA expression through epigenetic remodeling. Theranostics 13(8): 2568-2582.
- 15. Zhao Y, Zhang H, Li R (2024) The STAT3/miR-124-3p regulatory axis in hepatocellular carcinoma: a novel therapeutic target. Signal Transduct Target Ther 9(1): 124.

Advanced Research in Gastroenterology & Hepatology



This work is licensed under Creative Commons Attribution 4.0 License **DOI**: 10.19080/ARGH.2025.22.556079

Your next submission with JuniperPublishers will reach you the below assets

- Quality Editorial service
- Swift Peer Review
- Reprints availability
- E-prints Service
- Manuscript Podcast for convenient understanding
- Global attainment for your research
- Manuscript accessibility in different formats (Pdf, E-pub, Full Text, audio)
- Unceasing customer service

Track the below URL for one-step submission

https://juniperpublishers.com/online-submission.php